

Mechanical Properties of the A359/SiCp metal matrix composite at wide range of strain rates

Wojciech MOĆKO^{1, a}, Zbigniew L. KOWALEWSKI^{2, b}

¹ Motor Transport Institute, Jagiellońska 80, 03-301 Warsaw, Poland

² Institute of Fundamental Technological Research, ul. Pawińskiego 5B, 02-106 Warsaw, Poland

^a wojciech.mocko@its.waw.pl, ^b zkowalew@ippt.gov.pl

Keywords: MMC, high strain rate, compression test, SiCp, aluminium alloy.

Abstract. The paper presents constitutive model of the aluminium metal matrix composite reinforced by a silicon carbide. Developed equation includes an empirically estimated term which takes into account softening effects of the composite due to reinforcement damages at a large strain. Experimental investigation of the aluminium based MMCs reinforced by silicon carbide of volume fraction equal to 0%, 10%, 20% and 30% were carried out. Tests were conducted at wide range of strain rates and large magnitudes of strains. Comparison between experimental and predicted data shows that the elaborated model may be applied for composite materials in computer simulations of large deformations.

Introduction

The SiC particles reinforcing metal-matrix composites (MMCs) exhibit higher strength than the corresponding base material. Therefore, they are often used in many practical applications such as brake rotors, suspension arms, housings, brackets, etc. All these elements are working mainly at various operating conditions where variations of temperature, loading types, and strains are observed. Therefore, the knowledge of constitutive behaviour of MMCs is of great importance for an accurate process design. It has to be noticed however, that it is very difficult or even impossible to formulate an universal constitutive law which covers at least one type of a metallic composites (e.g. aluminium based composites). Such problems appearing due to variety of different reinforcement shapes and distributions, volume fractions and particle shapes which result from different methods of material fabrication.

At static loading conditions many experimental investigations concerning mechanical properties determination of MMCs have been carried out. The effects of material parameters such as reinforcement volume fraction, size, shape and particle distribution on plastic deformation and failure mechanisms were extensively studied [1-3] and as a result one can conclude that mechanical response of MMCs is well known. This is not true, and therefore, further intensive investigations are necessary. In the case of theoretical and numerical investigations two different approaches might be applied in order to describe a static deformation process of MMCs. The first is based on continuum plasticity [4-7] and gives reasonable results for composites containing particles larger than 10 μ m. The second method is based on dislocation plasticity model [7, 8], but it might be applied only in the case of sub-micron and small concentrations of the reinforcement particles. To reduce a gap (for particles from 0,1 μ m to 10 μ m) between proposed approaches, a hybrid model was introduced which connects effective intermediate approach with essential features of dislocation plasticity [9].

Experimental and theoretical characterizations of mechanical response of MMCs at high strain rates are still very attractive for many research centers. This is because of problems arising during description of damage development and deformation mechanisms due to variety of dynamic loading techniques, processing methods, and material types. Although many publications concerning dynamic behaviour of MMCs are devoted to either experimental [10-13] or theoretical [14-16] aspects, only some of them are trying to solve existing problems simultaneously by both types of analysis.

Hence, the objective of this study was to investigate experimentally a mechanical response of aluminium MMCs over a wide range of strain rates and different volumes fraction of reinforcement, and to develop a reasonable constitutive equation for large strains. The investigated MMCs were the Duralcan F3S.X0S type alloys. As a reference matrix material, the A359 alloy was used. Chemical composition of the materials is shown in Table 1.

Table 1. Chemical composition of the MMCs.

Alloy	Chemical composition % wt.								
	Si	Fe	Cu	Mn	Mg	Zn	Ti	Al	SiC
A 359	8,58	0,12	0,03	-	0,46		0,11	rest	-
F3S.10S	8,88	0,07	0,001	0,002	0,62	0,002	0,10	rest	11,3
F3S.20S	9,2	0,12	<0,01	0,02	0,54	<0,01	0,10	rest	20,8
F3S.30S	9,3	0,18	0,01	0,02	0,56	<0,01	0,11	rest	29,5

Experimental methodology

Quasi-static compression tests were performed on the Instron 8802 servo-hydraulic testing machine (Instron), at room temperature, and using two strain rates: $5 \times 10^{-4} \text{ s}^{-1}$ and 10^{-2} s^{-1} . The electro-mechanical extensometer was applied for strain measurements.

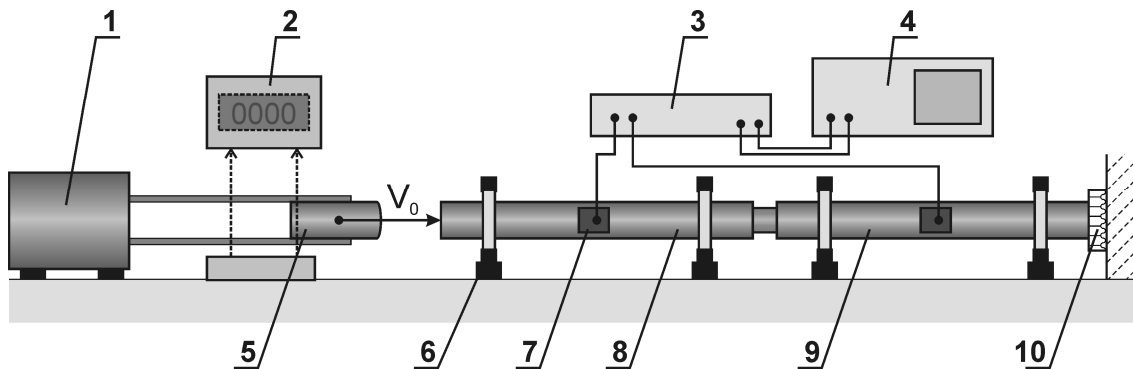


Fig.1. Diagram of the SHPB testing stand, 1 – air gun; 2 – striker velocity measurement; 3 – SG bridge and amplifier; 4 – digital recorder; 5 – striker bar; 6 – support; 7 – strain gauge; 8 – incident bar; 9 – transmitter bar; 10 – damper.

The dynamic compression [17, 18] experiments under high rates of deformation were carried using the SHPB apparatus [19] for the average strain rate equal to $2,6 \times 10^3 \text{ s}^{-1}$ at room temperature. A diagram of the conventional SHPB testing stand is presented in Fig.1. The specimen is placed between incident and transmitter bars. When striker bar impacts the incident bar a rectangular stress pulse is generated and travels along the incident bar until it hits the specimen. Part of the incident stress pulse gets reflected from the bar/specimen interface because of the material impedance mismatch, and part of it is transmitted through the specimen. The transmitted pulse emitted from the specimen travels along the transmitter bar until it hits the end of the bar. The stress, strain and strain rate in the specimen can be calculated from the recorded strains of two bars, in the following way:

$$\delta = E \left(\frac{A}{A_S} \right) \varepsilon_T \tag{1}$$

$$\varepsilon = -\frac{2C_0}{L} \int \varepsilon_R dt \tag{2}$$

$$\dot{\varepsilon} = \frac{d\varepsilon(t)}{dt} = \frac{-2C}{L} \varepsilon_R(t), \tag{3}$$

where: E – elasticity modulus of the Hopkinson bar, A – cross-section area of the bar, A_S – cross-section area of the specimen, C_0 – longitudinal wave velocity, L – specimen length.

Specimens for metallographic examinations were extracted from testpieces used at dynamic tests by means of precision cutting machine and polished applying STRUERS equipment. Specimens were prepared according to the typical method usually applied for aluminium alloys and silicon carbides reinforced composites. Optical micrographs were obtained using OLYMPUS PMG3 microscope equipped with the computer image analyzer.

Results

Mechanical response of the reference matrix material (A359 alloy) is shown in Fig. 2. It contains the results of: static tests obtained applying servo-hydraulic testing machine at the strain rates of 10^{-4} and 10^{-2} s^{-1} ; SHPB dynamic tests carried out at the strain rate of $6 \times 10^3 \text{ s}^{-1}$, and experimental data of Li and Ramesh [20] measured using pressure-shear plate impact at a deformation rate of $1,1 \times 10^5 \text{ s}^{-1}$ and $1,8 \times 10^5 \text{ s}^{-1}$. The entire range of strain rates in question covered magnitudes from 10^{-4} s^{-1} up to $1,8 \times 10^5 \text{ s}^{-1}$. The matrix material shows clearly visible strain hardening effect independently of the deformation rate. Moreover, the strain rate hardening effect can be observed. Strain rate sensitivity of the matrix material is presented in Fig. 3. The same type of effects is also illustrated in Fig. 7 for the F3S.20S MMC at various strain rates. In comparison to the reference matrix material, a stress level at the composite is significantly higher for the same magnitudes of strain and strain rate. It has to be emphasized however, that the composite does not exhibit greater hardening effect than that at the matrix material observed.

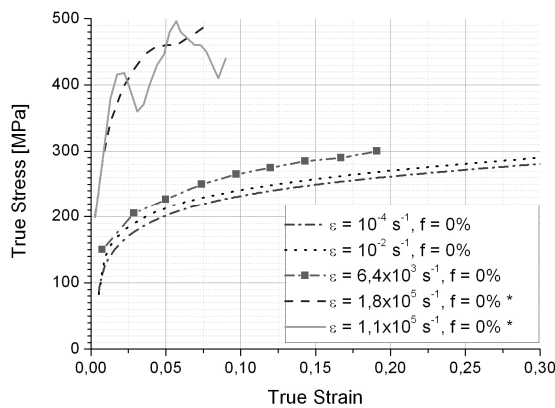


Fig. 2. Stress-strain curves of matrix material at various rates of deformation. *) – Li, Ramesh data.

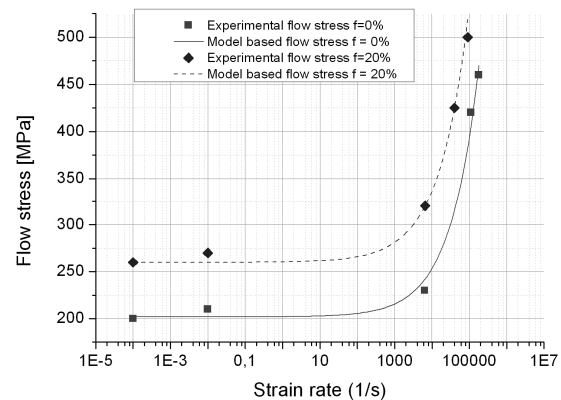


Fig. 3. Strain rate sensitivity of the A359 matrix

An analytical model for mechanical response of MMC can be expressed using the following equation [20]:

$$\delta(f, \varepsilon, \dot{\varepsilon}) = \delta_0(\varepsilon) g(f) \left(1 + \left(\frac{\dot{\varepsilon}}{\dot{\varepsilon}_0} \right)^m \right) \left(1 + A \left(\frac{\dot{\varepsilon}}{\dot{\varepsilon}_0} \right)^m f \right) \quad (4)$$

where $\delta_0(\varepsilon)$ represents the stress-strain characteristic of the matrix at quasi-static rates of deformation; $g(f)$ represents the variation of the flow stress ratio with volume fraction f ; A , m and $\dot{\varepsilon}_0$ are parameters which determine the rate sensitivity of the matrix material. Theoretical predictions according to Eq. 4, will properly characterize strain rate hardening effects at low magnitudes of strains. In the case of large strain levels (above 0,05) the hardening effects are

relatively well represented only for the matrix material. For the composite a predicted flow stress is significantly higher than that from test obtained. It may be concluded that such mechanical behavior of the composite is connected with damage development process of the silicon carbide reinforcement grains [21, 22]. The reason of such behavior is compressive deformation process of the reinforcement phase which results in exceeding the fracture strength of some, mainly large, grains. Proportion of particle fractures increases with increasing strain imposed into the composite, hence a scatter between prediction and experimental data increases with strain magnitude increase and reinforcement volume as well.

Fig. 4 illustrates optical micrograph of the as-received composite reinforced with 20% silicon carbide. It consists of α solid solution in which eutectic separations as well as reinforcement grains are placed. Reinforcement grains of different diameter are non-uniformly dislocated across material. Average Feret diameter is equal $5\mu\text{m}$ with standard deviation value of $6\mu\text{m}$, thus sizes of grains varies very significantly.

After deformation under static loading conditions a fragmentation of the reinforcement particles may be observed, Fig. 5. The silicon carbides are strongly fragmented and crushed. However, direct comparison of the as-received and prestrained specimens is difficult because of random and non-uniform displacement of the eutectic and reinforcement grains across material.

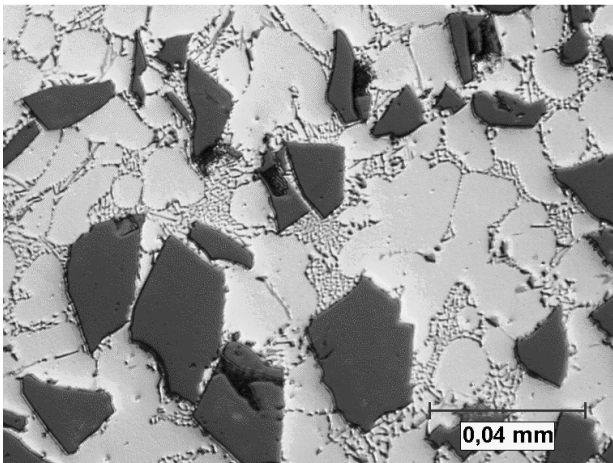


Fig. 4. Cross-section of the as-received F3S.20S composite (SiCp = 20%).

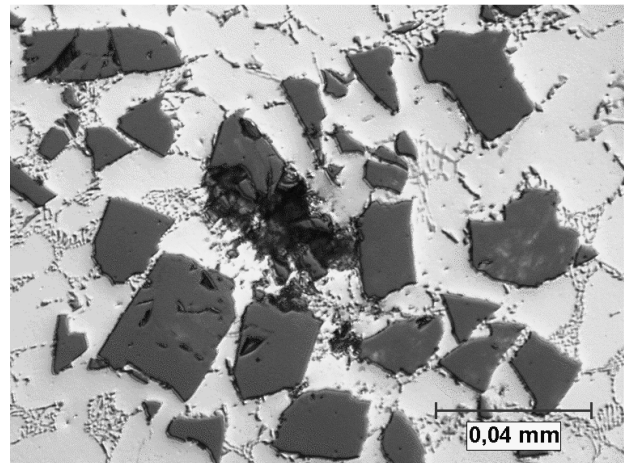


Fig. 5. Transversal cross-section of the F3S.20S composite (SiCp = 20%) after deformation under static loading.

In order to incorporate effects of the reinforcement damage into general equation describing composite mechanical response, it was assumed that softening effects caused by grains damage are proportional to strain and reinforcement volume fraction. It can be expressed by the following relationship:

$$\delta(\varepsilon, f) = \delta_c (1 + A\varepsilon)(B + fC) \quad (5)$$

where δ_c denotes flow stress of the composite calculated according to Eq. 4.

On the basis of experimental results all parameters of Eq. 5 were determined, i.e.: $A = -0,6$; $B = 0,96$; $C = -0,1$. Comparison of the corrected model predictions with experimental data is shown in Fig. 6. The model gives much better results at large strain, than the model without damage effects correction (Eq. 4), however it underestimates magnitudes of the flow stress at strains less than 0,1. It can be assumed that for such computer simulation purposes in which large deformation are taken into account the proposed model is good enough to obtain reliable predictions.

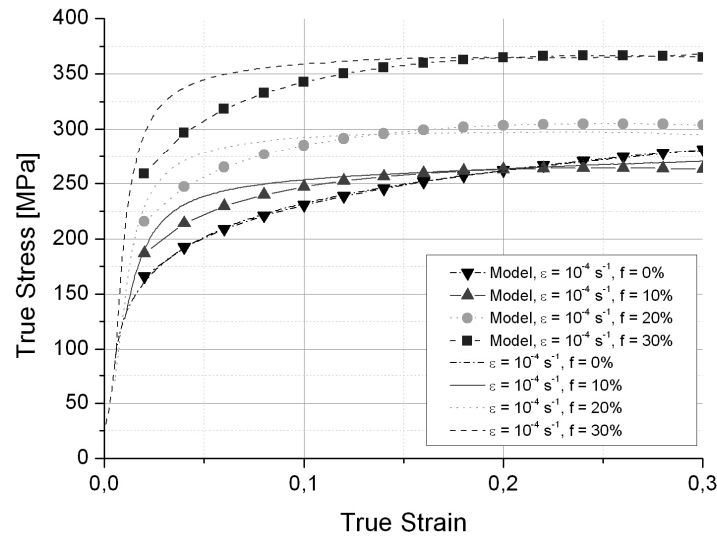


Fig. 6. Comparison of the experimental and predicted data for the A359 matrix and composite material reinforced by SiC of 10%, 20% and 30% volume fraction under static loading conditions.

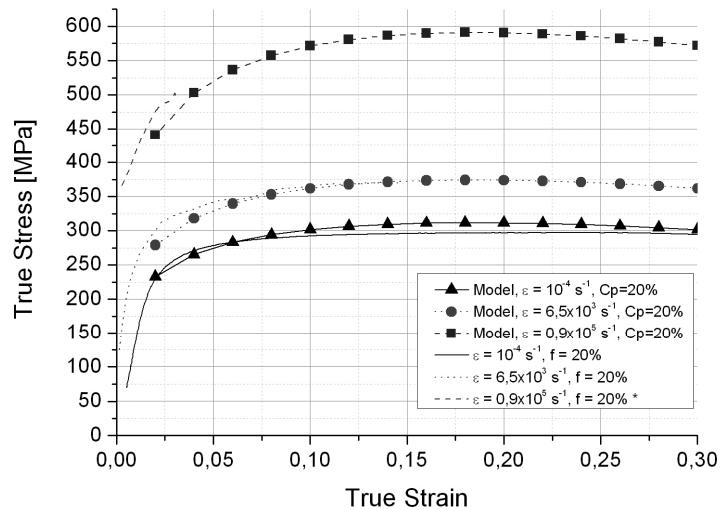


Fig. 7. Comparison of the experimental and predicted data for the composite material reinforced by 20% volume fraction of SiC at various strain rates.

Comparison of the experimental and calculated data according to Eq. 5 is shown in Fig. 7. Theoretical predictions slightly underestimates a flow stress at a low magnitudes of strain (under 0,05), however at higher strain values they fits experimental data correctly. Mutual relationship between the strain rate hardening and deformation rate is estimated properly for the composite tested in this research.

Conclusions

Experimental investigations were carried out in order to capture stress-strain curves of the composite over a wide range of strain, strain rate using four levels of reinforcement volume fraction. The experimental results were compared with data calculated by means of the model represented by Eq.4. Predicted data well describe the reference matrix material (SiCp=0%), whereas those achieved for the composite material, overestimated significantly the magnitude of flow stress. As it is

presented in this paper, the reasons of such scatter coming from the softening effects induced due to damage development of the reinforcement particles. Images from the optical microscope investigations clearly show damage of reinforcement grains in the prestrained material. In order to take into account the softening effects due to reinforcement particles damage, an additional term (Eq. 5) was introduced. Such correction assumes that softening effects are linear function of strain and reinforcement volume fraction. The correction enabled a significant reduction of the overestimations during calculations. It has to be emphasized that the model is suitable for computer simulations of large deformations.

References

- [1] T. Christman, et al., *Acta Metall.*, 37 (11), (1989), p. 3029.
- [2] A. G. Evans et al., *Scripta Metall. Mater.*, 25, (1991), p. 3.
- [3] J. Yang, et al., *Acta Metall. Mater.*, 39 (8), (1991), p. 1863.
- [4] Y.P. Qiu, G.J. Weng, *Int. J. Solids Struct.* 27, (1991), p.1537.
- [5] S.F. Corbin, D.S. Wilkinson, *Acta Metall. Mater.* 42, (1994), p. 1131.
- [6] G. Bao, J.W. Hutchinson, R. M. McMeeking, *Acta Metall. Mater.* 39, (1991), p. 1871.
- [7] M.F. Ashby, *Phil. Mag.* 14, (1966), p. 1157.
- [8] F.J. Humphreys, in: *Dislocations and Properties of Real Materials*, p. 175. Inst. of Metals, London, 1985.
- [9] C.W. Nan, D.R. Clarke, *Acta Mater.* 44, (1996), p. 3801.
- [10] D.P. Dandekar, C. M. Lopatin, in: *Shock Waves in Condensed Matter*, 1985, ed. Y.M. Gupta. Plenum, New York, 365-369, 1986.
- [11] C.M. Friend, A.C. Nixon, *J. Mater. Sci.*, 23, (1988), p.1967.
- [12] D.G. Dixon, *Scripta Metall. Mater.*, 24(3), (1990), p. 577.
- [13] S. J. Bless et al., in: *Shock-Wave and High-Strain-Rate Phenomena in Materials*, ed. M.A. Meyers, L.E. Murr and K.P. Staudhammer, Marcel Dekker, New York, 1051-1058, 1992.
- [14] C.A. Ross, R.L. Sierakowski, in: *Materials 1971: Science of Advanced Materials and Process Engineering*, National SAMPE Symposium and Exhibition Vol. 16. SAMPE, Azusa, California, 109-121, 1971.
- [15] J. Harding et al., in: *Proc. 6th Int Conf. on Composite Materials (ICCM VI)*, Vol. 3 ed. F.L. Matthews et al. Elsevier Applied Science, London, 76-85, 1987.
- [16] A. Marchand, et al., *Engng. Fract. Mech.*, 30, (1988), p. 295.
- [17] E. D. H. Davies, S. C. Hunter, *J. Mech. Phys. Solids*, 11, (1963), p. 155.
- [18] U.S. Lindholm, L. M. Yeakley, *J. Mech. Phys. Solids*, 13, (1965), p. 41.
- [19] U.S. Lindholm, *J. Mech. Phys. Solids*, 12 (5), (1964), p. 317.
- [20] Y. Li, K.T. Ramesh, *Acta Mater.* 46, (1998), p. 5633.
- [21] D.J. Lloyd, *Int. Mater. Rev.* 39, 1, (1994).
- [22] W.H. Hunt, Jr, J.R. Brockenbrough, P.E. Magnusen, *Scripta Metall. Mater.* 25, (1993), p.15.

Performance, Protection and Strengthening of Structures under Extreme Loading
10.4028/www.scientific.net/AMM.82

Mechanical Properties of A359/SiCp Metal Matrix Composites at Wide Range of Strain Rates

10.4028/www.scientific.net/AMM.82.166